Astron. Astrophys. 320, L13–L16 (1997)

ASTRONOMY AND ASTROPHYSICS

LETTER

Letter to the Editor

Return current effects on hard X-ray and microwave emission produced by electron beams in solar flares

V.V.Zharkova[1] **and D.V.Syniavskii**[2]

[1] Department of Physics and Astronomy, University of Glasgow, Glasgow G12 8QQ, Scotland, U.K.
[2] Physics Department, Kiev University, Kiev, 252022, UKRAINE

Received 24 September 1996 / Accepted 21 January 1997

Abstract. Electron beam distribution functions, found from a joint solution of the kinetic and electric current conservation equations for an electron beam in converging magnetic field, are used for the calculations of resulting hard X-ray bremsstrahlung fluxes for beams with different parameters. X-ray fluxes are shown to have non-monotonic energy distributions with the flux depression (dip) at 20-25 keV, caused by the effect of an electric current on the beam electron distributions, with spectral indices before the dip higher by 1-1.5 units than after it. These effects can explain surprisingly well the observational discrepancies in spectral indices and total energy fluxes, detected from SMM and Yohkoh hard X-ray observations in different energy bands.

Key words: Sun: flares– Sun: x-rays– plasmas – electron beams

1. Introduction

An interpretation of simultaneous observations on board of the SMM satellite of impulsive solar events in different hard X-ray bands (MacKinnon *et al.* (1985), Duijveman *et al.* (1982)) and in microwave emission (Kosugi (1986), Schmahl *et al.* (1986)) revealed some discrepancies in the explanation by a pure collisional model of electron beam precipitation. The footpoint X-ray fluxes, obtained by HXIS in a range of 16-30 keV, were found to be only 15-28 % of the fluxes, extrapolated to the same energy range from the HXRBS spectra, observed at higher energies of 25-300 keV. A possibile flattening of the spectrum at energies below 30 keV could explain this result, but the HXIS emission has much bigger spectral index than the HXRBS spectrum.

Similar time profiles of X-ray and microwave emission are likely to be provided by a common particle acceleration, but there is a noticeable decrease (up to 3 orders of the magnitude) in total microwave fluxes, than those in X-rays. This allows to suggest that microwave emission is caused by higher energy electrons with $E \geq 200$ keV, whose abundance is 3 orders of magnitude lower than those for lower energy electrons. From comparison of hard X-ray emission, obtained by HXRBS, and microwave radiation, observed by VLA, the hard X-ray indices are higher by 1-2 units than those deduced from microwaves (see Kosugi, (1986, and Schmahl *et al.* (1986)). More recent observations with the Nobeyama Radioheliograph and their comparison with the Yohkoh Hard X-ray Telescopes, done by Nishio *et al.* (1995), led to similar conclusions. An interpretation of microwave and hard X-ray observations by non-thermal electron beams in a pure collisional approach showed that the microwave spectra normally are flatter (harder) by 1-2 units than those derived from hard X-rays.

In order to understand these discrepancies, more advanced kinetic simulations were required and these have been carried out in the past decade. An electron beam dynamics was considered taking into account anisotropic scattering in electric (Diakonov and Somov (1988, Emslie (1980)) and converging magnetic fields (Karlicky *et al.*, (1990, Leach and Petrosian (1981), McClements (1992), Syniavskii and Zharkova (1994), Zharkova *et al.* (1995)). In collisional model with Ohmic heating, return current energy losses in the fully ionised coronal plasma were shown to have a noticeable effect on the injected beam dynamics in depth, particularly at the chromospheric level (Emslie (1980)). They reduce a penetration distance of beam electrons, responsible for bremsstrahlung emission, and, therefore, increase total energy flux, required for the production of this emission (LaRosa and Emslie (1988), Diakonov and Somov (1988)).

The return current losses were overestimated in the partially ionized ambient plasma taking into account anisotropic scattering, and were found to vary strongly in depth (Syniavskii and Zharkova (1994, hereafter Paper 1). At low coronal and upper chromospheric levels, where the ambient plasma is completely ionised, the induced electric field governs completely an injected beam dynamics. Less powerful beams with smaller upper energy limit do not precipitate to the chromosphere, but lose their energy at higher levels, transforming into electrons of return current with nearly a Maxwellian distribution. More

Send offprint requests to: V.V.Zharkova

powerful beams precipitate to chromospheric levels with wider angular distributions and smaller abundances of low energy electrons than in the initial beams. These results emphasize the importance of return current effects, but still could not give an explanation of the observational discrepancies.

A self-consistent solution of the equation for induced electric field and of kinetic equation, for beam electrons with anisotropic scattering in a presence of electric and converging magnetic fields (Zharkova *et al.* (1995), confirmed the previous results for coronal levels. But at the transition region and chromosheric levels, where the ambient plasma is partially ionized, the return current effect was considerably decreased. It results that the full electron beam thermalization, caused by return current, is occurred at lower column depth but at higher upper energy limit $E \leq 150keV$. At the chromospheric level, instead of the steep fall at lower energies found in the model with collisions and Ohmic losses, electron distributions revealed an energy depression (dip) at lower energies (22-25 keV) which divides electron energy distributions into 2 parts. Before the dip ($E \leq 20keV$) the energy distributions have a single power law, but with higher spectral indices than the initial ones. The dip is followed by maximum with nearly normal distribution, and after the dip, at higher energies ($E \geq 30keV$), the distributions have a power law again with the initial spectral indices.

As it was shown by Emslie and Smith (1984)) these energy distributions with maximum in tail can be two stream unstable with consequent generation of Langmuir waves. However, in our models this instability takes place only for very intensive beams, and it will be discussed in Section 3.2.

In the present paper we apply the electron distributions from Paper II to the interpretation of the observational features, which can be associated with the kinetic effects of electron beam precipitation.

2. Observational features

Let us briefly summarise the main observational discrepancies found from the SMM and Yohkoh observations and their comparison with microwave observations.

2.1. Hard X-ray emission

A comparison by MacKinnon *et al.* (1985) of hard X-ray fluxes for a few flare events, observed by the Hard X-ray Imaging Spectrometer (HXIS) in energy band of 16-30 keV and by the Hard X-ray Burst Spectrometer (HXRBS) in a range of 25-300 keV range aboard the Solar Maximum Mission, systematically showed the following discrepancies:

- 16-30 keV HXIS footpoint fluxes in a few flares were about $15 - 30\%$ of the simulteneous HXRBS flare fluxes, extrapolated by a power law into this lower energy range;
- footpoint spectra for some flares are much softer than the HXRBS; the difference between the spectral indices is about 1-2 units which cannot be considered as the observational errors.

2.2. Microwave emission

- the energy distributions of electrons, producing a burst emission, were found to have a power law with a spectral index equal to 3.2, whereas the simultaneous hard X-ray observations gave a spectral index equal to 5;
- the total number of electrons (10^{33}), producing microwave emission, is systematically lower by three orders of magnitude, than the total number of electrons (10^{36}) responsible for hard X-ray emission.

3. Simulational results and discussion

3.1. Electron beam distributions

For an explanation of the observational discrepancies in hard X-ray and microwave emission we used the results of Paper II. An electron beam was assumed to be injected within 6 s with a power law in energy and Gaussian profiles in pitch angle cosines and time. The loop was considered to have a closed configuration with converging magnetic field, the beam electrons are assumed to be scattered anisotropically into both negative and positive pitch angles, inducing the electric field of return current. A temperature, density and macrovelocity of the ambient plasma were considered to result from a hydrodynamic response to the beam input, and ionization was governed by the hydrogen ionization.

3.1.1. Energy and angular distributions

Some of the beam electron distribution functions calculated for different depths, energy and pitch-angle cosines are plotted in Figure 1 (Paper II), where the dimensionless energy z is equal to 1 at energy of 15 keV, to 2 - at 30 keV etc.

Most important simulated features, obtained from the kinetic solutions for beam electrons, are the following:

- A return current effect appears mostly at the transition region where a strong beam dissipation is caused by Ohmic heating of the ambient plasma (see Figure 1 (b,c) and Figure 2 in Paper II).
- Powerful and hard electron beams with $F_0 \geq 10^{11} - 10^{12} erg/cm^2/s$ and $\delta = 4$ produce higher induced electric field of return current and, therefore, more low energy electrons, moving backward to the source in the corona.
- Softer and less powerful beams which have smaller upper energy limit ($\leq 150keV$) and wider initial angular distributions (Figure 2 in Paper II), can be thermalized completely at the transition region, transforming into secondary beams moving backwards with nearly normal distribution in energy.
- A residual part of the initial beam electrons with higher energy ($\geq 150keV$) still can precipitate down to the photosphere as a beam with a power law in energy, but with narrower energy range and wider angular distributions.
- The secondary beam of return current, returning to the source, causes a split in energy of initial beam. At the transition region, for harder beams, it results in a dip at 20-25 keV in energy distributions followed by maximum at 30-35

keV. After maximum the electron distributions have a single power law in energy with the initial spectral indices. For softer beams there is even a single maximum at 30-35 keV in the energy distributions with a fall of electron abundances in both lower and higher energy tails.

– If electron beams are powerful enough to precipitate down to the photosphere, the dip disappears completely at the chromospheric level. But the abundances of low energy electrons increase in depth, and electron energy distributions become steeper than the initial ones, or their spectral indices become higher. It results in softening of initial beams during their precipitation into the deeper chromosphere.

3.1.2. X-ray bremsstrahlung emission

The hard X-ray bremsstrahlung flux was calculated from the beam electron distribution functions $f(z, \mu, s, t), electron/cm^3$ at the viewing angle ψ, as the following:

$$F(E,\psi) = 2\pi A_x \int_0^1 \int_E^{100} \int_{s_{min}}^{s_{max}} d\mu z\, dz ds\, n f(z,\mu,s,t) \qquad (1)$$
$$\left(d\sigma_{\parallel}^B(E,z,\psi) + d\sigma_{\perp}^B(E,z,\psi) \right),$$

where $A_x = I_0 \frac{S}{4\pi R^2}$, I_0 is an intensity unit from paper by Nocera *et al.* (1985), μ - pitch angle cosine, n - ambient plasma density, S is the area of flare, and R is the distance from an observer. The scattering cross-sections in the directions being parallel and perpendicular to magnetic field, $d\sigma_{\parallel}^B$ and $d\sigma_{\perp}^B$, as well as the variables z, s, s_{min} and s_{max} were taken from Paper II.

In Figure 1 there are plotted hard X-ray fluxes calculated for electron beam distributions with viewing angle $\psi = 90^0$ from Paper II (Figures 1 and 2), (a) - for harder and more intensive beam with $\delta = 4$, $F_0 = 10^{11} erg/cm^2/s$ and (b) - for softer and weeker beam with $\delta = 7$, $F_0 = 10^{10} erg/cm^2/s$. The energy range of hard X-ray fluxes of 15-300 keV (z=1-20) covered both the HXIS and HXRBS energy bands.

The hard X-ray energy distributions reflect rather complicated energy distributions of beam electrons caused by the kinetic effects of beam precipitation. The main features, found from the hard X-ray energy distributions, are:

– Despite the integration over pitch angles and electron energies, similarly to electron energy distributions, harder and more intensive X-ray fluxes (Figure 1a) have a dip at 20-25 keV in flux energy distributions followed by maximum at 25-30 keV. The dip is smaller than those in the electron distributions but still well pronounced.

– Energy distributions after the dip retain initial spectral indices, whereas at lower energies, before the dip, the spectral indices are higher than after it, or the fluxes are much softer than those at higher energies.

– X-ray flux in Figure 1(b), caused by softer and weaker beams with upper energy limit of 300 keV, shows flattening in the energy distributions at the slightly higher energies of 24-27 keV. The index before this flattening is higher than the initial one, whereas after flattening the distribution is similar to the initial one.

– If the upper energy limit of electron energy is smaller (150 keV), the flux distribution becomes more flattened, or harder, than initial electron distribution, but at 27-28 keV the flux again reaches the initial spectral index.

– X-ray fluxes, calculated in Figure 1(a,b) from 30 keV to lower energies for pure collisional electron distributions with the same spectral indices as after the dip, are much higher, than the one, calculated for more sophisticated distributions with the dip. Consequently, for these distributions the total X-ray fluxes, calculated as an integral in energy range of 15-300 keV, are lower by 60-70 % than those obtained for a pure collisional model with single power law.

3.2. Discussion

Let us compare the observations of hard X-ray fluxes in different energy bands, discussed in Section 2, with the simulations which can explain the discrepancies in interpretation surprisingly well.

In the present kinetic model electron beams are found to be thermalised completely if their upper energy limit is $\leq 150keV$ for softer beams and even higher for harder beams. For beams to be able precipitate down to the chromosphere, a higher upper energy limit ($\geq$180 keV) is required. This is very close to the energy limit of 200 keV, deduced for X-rays and microwaves by McKinnon *et al.* (1985). The abundances of electrons with energies higher than 200 keV, deduced from the electron distribution functions in Paper II, are dramatically decreased in depth by the return current effect. But even at the injection site the ratio of electron abundances with energies below and higher 200 keV is about 4 orders of magnitude. An integration in depth, used in the observational interpretation, results in the ratio of about 3 orders of magnitude, which matches those deduced by Koshugi (1986) and Nishio *et al.* (1995) from hard X-ray and microwave observations.

The energy limit in simulations is assosiated with the effect of induced electric field and can be even higher, if the electrons are injected not along magnetic field lines but at bigger pitch angles. Less energetic electrons lose their energy mainly in the corona and transition region, producing the observed hard X-ray emission. More energetic electrons can precipitate down to the chromosphere, losing their energy in Ohmic and collisional losses with ions and neutrals with a production of the observed microwave emission. Owing to wide pitch angle distributions in depth, the electrons, responsible for this emission, can be taken to be isotropic (McKinnon *et al.* (1985)).

Let's evaluate the parameters under which a two stream instability, destroying such distributions by a quasi-linear relaxation and, in turn, causing Langmuire waves, denoted by Emslie and Smith (1984)), will take place in our models. There are two kinds of the beam pairs which can produce the instabily: a direct electron beam and ambient plasma electrons as well as the direct beam and the beam of return current.

For the first pair to comply with the beams instability criteria (formula (14) in the paper by Emslie and Smith (1984)),

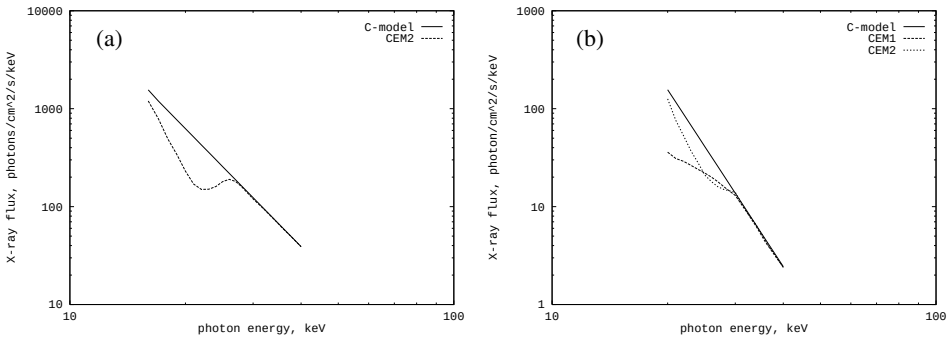

Fig. 1. The hard X-ray fluxes caused by electron beams with the initial parameters $\delta = 4$, $F_0 = 10^{11} erg/cm^2/s$ (a) and $\delta = 7$, $F_0 = 10^{10} erg/cm^2/s$ (b), C denotes a pure collisional model with anisotropic scattering, CEM denotes a model with collisions, electric and converging magnetic fields; 1 refers to upper energy limit of 150 keV, 2 - 300 keV.

very powerful beams with initial energy fluxes $F_0 \geq 10^{12} erg \cdot cm^{-2} \dot{s}^{-1}$ are required, as in our models the dips followed by bump-in-tail appear at the depths $\xi = 1.7 \cdot 10^{19} cm^{-2}$, where an electron temperature is about 10^5 K and ambient plasma density is about $10^{12} cm^{-3}$.

For the second pair of beams: direct and return current beams, the situation is a little more complicated, as their abundances and energies are related each to other. Our preliminary estimations show that the instability criteria above is satisfied: at chromospheric levels - for any beam parameters and at coronal levels - for the beams with the initial flux $F_0 \geq 10^{11} erg \cdot cm^{-2} \dot{s}^{-1}$. We did not consider either of such beams in the present simulations, but we are planning to investig this problem in our future papers, as it is likely to explain some puzzles in microwave observations.

Therefore, we can conclude that in the presented models a particle-particle approximation can be used without a significant effect on the beam electron distributions.

The most difficult problem for a pure collisional model was to explain the difference in spectral indices, deduced from softer and harder ranges of X-ray and microwave observations. In the present kinetic model this difference is explained by a variable in depth action of the induced electric field of return current. This field causes a dip in electron energy distributions at 20-25 keV at the corona and transition region, which disappears at chromospheric levels, where, however, the electron distributions become softer.

The integration in depth of electron distribution functions leads to X-ray fluxes having depressions at the energies where electron distributions have dips. X-ray fluxes are also divided by these depressions in two parts: lower energy and higher energy ones. A lower energy part, with $E \leq 20 keV$, is shifted to lower energies by width of the dip (5-6 keV). Owing to integration of electron distributions in column depth, the lower energy fluxes have much softer energy distributions than the initial ones, which results from softening of electron energy distributions at chromospheric levels described above. Since a higher energy flux, $\geq$ 30 keV, is not affected by the induced electric field, so it has the same spectral index as in the initial distributions. The difference in spectral indices between lower and higher energy parts is about 1-1.5 which is comparable with those deduced from the observations.

From the explanations above, the difference in total X-ray fluxes, deduced from the HXIS (15-30keV) and from the extrapolated HXRBS (25-300 keV) observations are fairly understandable. Since the extrapolation of the HXRBS fluxes from 30 keV to lower energy range has been done in a pure collisional model, so the fluxes do not show the depression caused by Ohmic losses. Thus they are not shifted to lower energy and produce higher total X-ray fluxes, than those deduced from distributions with the depression. The difference between these total fluxes is about $65 - 75\%$ which is close to the ratios found from the observations.

Therefore, we can conclude, that the observational discrepancies arise from their interpretation by a pure collisional electron beam precipitation into the atmosphere. The more sophisticated kinetic approach considering anisotropic scattering of electron beams in the ambient plasma with partial ionisation in a presence of induced electric field of return current and converging magnetic field can give a reasonable explanation of such observations. And from the differences in total fluxes and spectral indices it should be possible to extract information about the magnitude of the induced electric field. This reinforces the point that the interpretation of hard X-ray and microwave emission requires more realistic kinetic models, which can provide more realistic pictures of electron beam dynamics.

References

Diakonov, S.V. and Somov, B.V., 1988, *Solar Phys.*, **116**, 119

Duijveman, A., Hoyng, P. and Machado, M., 1982, *Solar Phys.*, **81**, 137

Emslie, A.G., 1980, *ApJ*, **235**, 1055

Emslie, A.G. and Smith, D.F., 1984, *ApJ*, **279**, 882

Karlicky, M., Alexander, D., Brown, J.C. and MacKinnon, A.L., 1990, *Solar Phys.*, **129**, 325

Kosugi, T., 1986, Proc. of the NSO/SMM Simposium, 20-24 August 1985, ed. D.F.Neidig, 409

LaRosa, T.N. and Emslie, A.G., 1988, *ApJ*, **326**, 997

Leach, J. and Petrosian V., 1981, *ApJ.*, **251**, 781

Leach, J. and Petrosian V., 1983, *ApJ.*, **269**, 715

MacKinnon, A.L.., Brown, J.C. and Hayward J., 1985, *Solar Phys.*, **99**, 231

McClements, K.G., 1992, *A& A.*, **258**, 542

Nishio, M., Yaji, K., and Kosugi, T., 1995, *Book of Abstracts*, Conference on Radio Emission from the Stars and the Sun, 3-7 July 1995, Barcelona, Spain, 37

Nocera, L., Skrynnikov, Ju.I., and Somov, B.V., 1985, *Solar Phys.*, **97**, 81

Schmahl, E.J., Kundu, M.R., and Dennis, B.R. , 1986, Proc. of the NSO/SMM Simposium, 20-24 August 1985, ed. D.F.Neidig, 396

Syniavskii, D.V. and Zharkova, V.V., 1994, *ApJSS*, **90**, 729 (Paper I)

Zharkova, V.V., Brown, J.C. and Syniavskii, D.V., 1995, *A & A*, **304**, 284 (Paper II)